Journal of Hazardous Materials 489 (2025) 137586

Contents lists available at ScienceDirect

Journal of Hazardous Materials

journal homepage: www.elsevier.com/locate/jhazmat

# Seasonal variations and intercorrelations of polycyclic aromatic hydrocarbons, heavy metals and environmentally persistent free radicals in $PM_{2.5}$ in Ulaanbaatar, Mongolia

Shihan Wu [a,b], Ke Xin [a,b], Jing Chen [a,b,*], Narmandakh Dambajamts [c,d], Yuewei Sun [a,b], Jing Ai [a,b], Wei Ouyang [a], Bilguun Ulziibat [d,e], Enkh-Uchral Batkhuyag [c,f], Soyol-Erdene Tseren-Ochir [c,f]

[a] State Key Joint Laboratory of Environment Simulation and Pollution Control, School of Environment, Beijing Normal University, Beijing 100875, China
[b] Center for Atmospheric Environmental Studies, Beijing Normal University, Beijing 100875, China
[c] Laboratory of Environmental Chemistry and Geochemistry, National University of Mongolia, Ulaanbaatar 14201, Mongolia
[d] Department of Chemical and Biological Engineering, School of Engineering and Technology, National University of Mongolia, Ulaanbaatar 14201, Mongolia
[e] Institute of Geography and Geo-ecology, Mongolian Academy of Sciences, Ulaanbaatar 14201, Mongolia
[f] Department of Green Energy and Engineering, School of Engineering and Technology, National University of Mongolia, Ulaanbaatar 14201, Mongolia

## HIGHLIGHTS

- Coal burning for household heating in Ulaanbaatar led to extreme $PM_{2.5}$ pollution.
- Metal elements associated with dusts exerted significant health effects.
- Vehicular emission was the major source of EPFRs rather than coal burning.
- Co-emissions of PAHs and specific metals by vehicles generated EPFRs.

## GRAPHICAL ABSTRACT

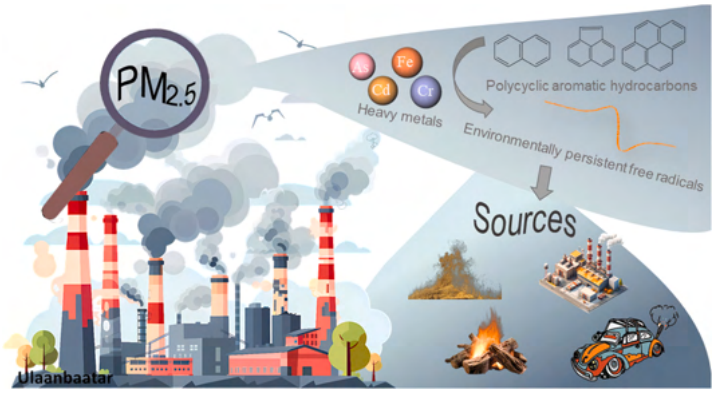


## ARTICLE INFO

*Keywords:*
PAHs
EPFRs
Domestic heating
Dust event
Health risk

## ABSTRACT

Simulated combustion experiments have identified polycyclic aromatic hydrocarbons (PAHs) and metal oxides as critical species in the formation of environmental persistent free radicals (EPFRs). However, little evidence exists regarding the interactions among PAHs, metals, and EPFRs in the real atmosphere. In this study, we collected $PM_{2.5}$ samples in downtown Ulaanbaatar in four seasons from 2020 to 2021, and analyzed the seasonal variations of 16 PAHs, 14 heavy metals and EPFRs in $PM_{2.5}$. The health risks of $PM_{2.5}$ were determined by calculating the incremental lifetime cancer risks of PAHs and heavy metals and equivalent cigarette numbers of EPFRs.

* Corresponding author at: State Key Joint Laboratory of Environment Simulation and Pollution Control, School of Environment, Beijing Normal University, Beijing 100875, China.
*E-mail address:* jingchen@bnu.edu.cn (J. Chen).

https://doi.org/10.1016/j.jhazmat.2025.137586
Received 26 November 2024; Received in revised form 20 January 2025; Accepted 10 February 2025
Available online 11 February 2025

According to the source apportionment results of the Positive Matrix Factorization (PMF) model, coal and biomass combustion, vehicular emission, and fugitive dust were identified as the dominant sources of PAHs, EPFRs, and heavy metals, respectively. The intercorrelations of EPFRs with PAHs and heavy metals from different sources revealed the important roles of most PAHs and some specific metals such as Zn, Pb, Sb, Sn, Tl in the formation of EPFRs. The dominant contribution of vehicular emission to EPFR pollution in $PM_{2.5}$ could be largely attributed to the co-emissions of PAHs and specific heavy metals in vehicular emission.

## 1. Introduction

A clear understanding of the composition, health risks and sources of $PM_{2.5}$ is a prerequisite for raising effective mitigation measures and improving air quality. Polycyclic aromatic hydrocarbons (PAHs) and heavy metals are two well-known groups of harmful components of $PM_{2.5}$, both of which contribute significantly to the health risks of $PM_{2.5}$ [1,2]. PAHs are typically generated from the incomplete combustion of carbonaceous materials, and most PAHs are carcinogenic and mutagenic to humans. Once emitted into the atmosphere, they can also migrate and transform in the environment, further generating more toxic products and secondary aerosol pollution [3,4]. On the other hand, heavy metals, among their various sources, can also originate from the combustion sources similar to those of PAHs. The coexistence of PAHs and heavy metals in $PM_{2.5}$ has been well documented in previous studies [5,6].

Environmentally persistent free radicals (EPFRs) are a new type of emerging pollutants that have attracted great attention in recent years [7]. EPFRs are a class of long-lived organic free radicals that can exist in the environment for tens of days or even months. EPFRs can be stabilized on atmospheric particulate matter and participate in atmospheric chemical reactions to form new pollutants [8]. Moreover, the inhaled EPFRs can catalyze the generation of reactive oxygen species in the human body, causing oxidative stress and consequently inducing aging and diseases [9]. High-temperature combustion of fossil fuels is an established formation process of EPFRs, in which EPFRs are produced via electron transfer between organic precursors and transition metals and stabilized on particles [10]. Besides, recent studies have also reported the formation of EPFRs under ambient conditions, through irradiation of atmospheric particulate matter by UV–visible light or heterogeneous reactions between ozone and aromatic organic precursors [7,11–13].

Simulated combustion experiments using model reactants have identified PAHs and metal oxides (CuO, ZnO, $Al_2O_3$, $Fe_2O_3$, etc.) as important precursors and surface catalysts for EPFR formation, affecting the yield, type and chemical lifetime of the generated EPFRs [9,14]. In addition, the formation of EPFRs upon irradiation of selected model PAHs further implied the crucial role of PAHs in producing EPFRs without metal oxides [15]. In fact, previous field investigation has revealed the strong correlation between PAHs and EPFRs [2]. However, very limited precursors were employed in previous simulation experiments either at high temperature or under ambient conditions. Besides, there are currently no field observation results exhibiting the interactions among PAHs, metals, and EPFRs in the real atmosphere, hindering the complete understanding of the roles of PAHs and metals in the formation of EPFRs.

Ulaanbaatar is located inland with a high altitude (1351 m above the sea level) and is one of the centers of the Siberian high. The minimum temperature in Ulaanbaatar can reach −40°C in winter and the maximum temperature can reach 35°C in summer, with an average annual temperature of around −1.5°C. Being the coldest inland capital city in the world, Ulaanbaatar suffers from severe $PM_{2.5}$ pollution due to the heavy use of solid fuels for heating in winter and frequent dust events in spring, and is ranked among the most polluted cities in the world according to World Air Quality Report. The incidence of respiratory diseases in Ulaanbaatar has increased dramatically in recent years, and the mortality rate due to indoor and outdoor pollution was estimated around one thousandth in 2016 [16,17]. Nevertheless, the chemical characteristics and health risks of $PM_{2.5}$ have been rarely studied, hindering the formulation and implementation of effective mitigation measures. In this study, we collected $PM_{2.5}$ samples in downtown Ulaanbaatar in four seasons between January 2020 and January 2021. The characteristics, health risks and sources of PAHs, heavy metals and EPFRs were simultaneously investigated, aiming for an effective mitigation of $PM_{2.5}$ pollution with regards to its health effects. Moreover, the greatly changing climate and $PM_{2.5}$ sources in Ulaanbaatar in four seasons enabled further exploration of the intercorrelations of the three toxic species, which helped to better elucidate the different roles of PAHs and heavy metals in EPFR formation.

## 2. Materials and methods

### 2.1. $PM_{2.5}$ sampling

$PM_{2.5}$ samples were consecutively collected for around half a month in each sampling period in January (winter), April (spring), July-August (summer), and October-November (autumn), 2020 and January, 2021 (winter) so as to capture the general changes of $PM_{2.5}$ in each season. Such sampling protocol has also been applied in previous studies investigating seasonal variations of $PM_{2.5}$ [41]. The sampling site in 2020 was on the roof of the four-floor main building of National University of Mongolia (NUM, 47.92°N 106.91°E), located in the city center of Ulaanbaatar. The sampling site in 2021 was shifted to another urban site near the Central Laboratory of Water and Sewerage Authority (47.92°N 106.94°E) due to the lockdown of NUM campus during the COVID-19 epidemic outbreak. All $PM_{2.5}$ samples were collected on pre-baked (450℃, 4 h) quartz filters (PALLFLEX, 25.4 × 20.3 cm) using a high-volume sampler at a flowrate of 1.05 $m^3 \cdot min^{-1}$. The sampling duration for each sample was 23.5 h from 8:30–8:00 the next day. A total of 82 effective $PM_{2.5}$ samples were collected in downtown Ulaanbaatar, including 17 in winter 2020, 14 in spring 2020, 15 in summer 2020, 21 in autumn 2020, and 15 in winter 2021. Before and after sampling, the filters were stabilized under constant temperature and humidity for 24 h and weighed by an analytical balance for three times. The sample filters were then stored in dark at −20 ℃ for further analysis.

Local meteorological conditions (temperature, wind speed, relative humidity) and common gaseous pollutant (CO, $SO_2$, $O_3$) concentrations were obtained from the nearby national environmental monitoring station. $NO_2$ concentration was continuously monitored in each sampling period by a nitrogen oxide analysis instrument (Thermo Fisher Scientific, 42I-DNMSDAA).

### 2.2. Sample analysis

PAHs: 2 $cm^2$ of each sample filter was cut and added with 100 μL of 1 μg $mL^{-1}$ hexamethylbenzene as a surrogate. The filter was then cut into pieces and ultrasonically extracted using n-hexane (10 mL) for three times. The combined extract was filtered with a 0.22-μm PTFE filter, and concentrated to 0.5 mL using ultrapure nitrogen gas. The concentrated solution was added with 10 μL of 100 ng $mL^{-1}$ internal standards and diluted to 1 mL for analysis by a Shimadzu triple quadrupole gas chromatography-mass spectrometer (GCMS-TQ8040). The internal standards for the GC-MS measurement included naphthalene-$D_8$, acenaphthene-$D_{10}$, phenanthrene-$D_{10}$, chrysene-$D_{12}$, and perylene-$D_{12}$. 16 PAH monomers were analyzed and the detection limit ranged from 0.02

to 0.22 ng $m^{-3}$. The recovery rates calculated by hexamethylbenzene were all above 90 % and the measured PAH concentrations were not corrected for recovery. The GC-MS analysis details are provided in the supporting file (Text S1).

Heavy metals: 12 $cm^2$ of each sample filter was cut into pieces and digested in 10 mL $HNO_3$-HCl digestion solution using a microwave. The digestion solution was prepared by diluting 55.5 mL $HNO_3$ and 167.5 mL HCl to 1 L with ultrapure water. The mixture was digested in the microwave at 180°C for 15 min. Afterwards, the mixture was filtered with a 0.45-μm PES filter, diluted to 25 mL with ultrapure water, and analyzed using a Shimadzu inductively coupled plasma mass spectrometer (ICPMS 2030). Li, Re, and Rh were selected as the internal standards (50 μg $L^{-3}$). The element signals were calibrated with 7-point calibration curves (0 μg $L^{-3}$, 1.0 μg $L^{-3}$, 5.0 μg $L^{-3}$, 10.0 μg $L^{-3}$, 25.0 μg $L^{-3}$, 50.0 μg $L^{-3}$, and 100.0 μg $L^{-3}$) and 14 heavy metal elements including As, Ba, Cd, Co, Cr, Cu, Fe, Mn, Ni, Pb, Sb, Sn, Tl, and Zn were measured.

EPFRs: EPFRs were measured using an electron paramagnetic resonance spectroscopy (EPR), which could detect the radical concentration, g-factor and line width (ΔHp-p) of EPFRs. Three 50 mm × 2 mm strips of each sample filter were neatly placed in one EPR tube and measured for EPFRs by an X-band EPR spectrometer (JOEL, JES-FA100, Japan). 2,2-diphenyl-1-picryhydrazyl (DPPH, 95 %) was applied as a standard radical for signal peak area calibration and EPFR concentration calculation. The detailed EPR operating parameters and procedure can be found in our previous study [7].

OC and EC: The organic carbon (OC) and elemental carbon (EC) contents of each sample were measured by a multi-wavelength carbon analyzer (Atmoslytic Inc., DRI Model 2015, USA). A punch of the sample filter (0.532 $cm^2$) was cut and analyzed by the carbon analyzer following the thermal/optical transmittance (TOT) protocol and IMPROVE-A temperature program [18]. The method detection limits (MDL) of OC and EC were 0.18 μg C $cm^{-2}$ and 0.04 μg C $cm^{-2}$, respectively.

### 2.3. Health risk assessment

The total carcinogenic equivalent concentration ($BaP_{teq}$) and mutagenic equivalent concentration ($BaP_{meq}$) of PAHs were calculated as follow:

$$BaP_{teq} = \sum_{i=1}^{n} PAH_i \times TEF_i \quad (1)$$

$$BaP_{meq} = \sum_{i=1}^{n} PAH_i \times MEF_i \quad (2)$$

where $PAH_i$ is the PAH monomer concentration, and TEFi and MEFi are the corresponding toxic equivalency factor (TEF) and mutagenicity equivalency factor (MEF), respectively [2]. The TEF and MEF values for individual PAHs are presented in Table S1.

The Incremental Lifetime Cancer Risk (ILCR) model was applied to evaluate the carcinogenic risks of PAHs and heavy metals via inhalation. The ILCR values of the target pollutants were calculated by Eq. 3.

$$ILCR = \frac{SF \times TEQ \times IR \times EF \times ED}{BW \times AT} \times 10^{-6} \quad (3)$$

Definitions of each parameter in Eq. 3 are as follow: *ILCR*: incremental lifetime cancer risk; *SF*: carcinogenic intensity coefficient of inhaled pollutants (PAHs: 3.85, As: 20.7, Cd: 6.3, Co: 9.8, Cr(VI): 42, Ni: 0.84, Pb: 0.28); TEQ: total equivalent concentration of PAHs or heavy metals, ng·$m^{-3}$; IR: respiratory rate, $m^3$ $d^{-1}$, which is 17.5 $m^3$ $d^{-1}$ for adult males, 14.5 $m^3$ $d^{-1}$ for adult females, and 10.9 $m^3$ $d^{-1}$ for children; EF: exposure frequency, 365 d $year^{-1}$; ED: exposure years, 30 years for adults and 18 years for children; BW: body weight, 66.1 kg for adult males, 57.8 kg for adult females, and 32.2 kg for children; AT: average exposure time of 25550 days, corresponding to 70 years of exposure [1,2].

The equivalent cigarette number was calculated to assess the exposure risk of EPFRs as follows [19]:

$$EQ_{cig} = (C_{EPFRs} \times V)/(RC_{cig} \times C_{tar}) \quad (4)$$

where $EQ_{cig}$ is the equivalent cigarette number (person$^{-1}$ day$^{-1}$), $C_{EPFRs}$ is the EPFR volume concentration in the atmosphere (spins $m^{-3}$), V is the inhaled volume of air by an adult per day, 20 $m^3$ $day^{-1}$, $RC_{cig}$ is the concentration of free radicals in cigarette tar, 4.75 × $10^{16}$ spins $g^{-1}$, and $C_{tar}$ is the tar concentration per cigarette, 0.013 g $cig^{-1}$.

### 2.4. Source apportionment by PMF

The sources of PAHs, heavy metals and EPFRs were analyzed using the Positive Matrix Factorization (PMF) 5.0 model released by the United States Environmental Protection Agency (US EPA). Duo to their unique emission characteristics from different sources and their stability in the atmosphere, PAH monomers and metal elements are often used as the source tracers of $PM_{2.5}$ in PMF [1,2]. In this study, the concentrations of the 16 PAHs and 14 heavy metals were collectively used as the inputs of the model to indicate source variation, and the total PAH concentration, total heavy metal concentration and EPFR concentration were set as the total variable, respectively, for apportioning their sources. The detailed PMF calculation and error estimation procedure is presented in our previous study [20].

The data uncertainty (Unc) can be calculated by Eq. 5 when the PAH or heavy metal concentration is above MDL, which was the case in this study. Besides, Unc can be calculated by Eq. 6 when the measured concentration is below MDL.

$$Unc = \sqrt{(Error\ fraction \times Concentration)^2 + (0.5 \times MDL)^2} \quad (5)$$

$$Unc = \frac{5}{6} \times MDL \quad (6)$$

### 2.5. Potential source region analysis by PSCF

The MeteoInfoMap software developed by China Meteorological Administration was used to conduct Potential Source Contribution Function (PSCF) analysis of $PM_{2.5}$ as well as backward trajectory clustering in Ulaanbaatar in each sampling period. Ulaanbaatar (47.92°N, 106.91°E) was set as the starting point of backward trajectories, with 48-hour backward tracking of air parcel trajectories at a height of 500 m and a time resolution of 1 hour. The study domain was divided into grid cells with a resolution of 0.5° × 0.5°. PSCF provides a preliminary assessment of the potential source regions by counting the number of air parcel trajectories in each grid cell with the $PM_{2.5}$ centration over a certain value. For detailed calculation steps, please refer to the previous study [21].

## 3. Results and discussion

### 3.1. Seasonal variations of toxic pollutants in $PM_{2.5}$ and their health risks

#### 3.1.1. Seasonal variations of $PM_{2.5}$ and the major components

The temporal variations of the concentrations of total PAHs (∑16 PAHs), total heavy metals (∑14 HMs), EPFRs, as well as OC and EC bound on $PM_{2.5}$ in Ulaanbaatar in the five sampling periods in 2020–2021 are shown in Fig. 1 and their mean concentrations in each sampling period are shown in Table 1. Overall, Ulaanbaatar was severely polluted with $PM_{2.5}$ in most seasons except for summer. While the $PM_{2.5}$ concentration was generally high in the cold seasons, spring showed the highest mean concentration of $PM_{2.5}$ (227.5 μg $m^{-3}$), which was attributable to the occurrence of dust events [8]. Also due to the high contribution of dust, the total heavy metal concentration was high in spring and autumn. The carbonaceous species in $PM_{2.5}$ (OC, EC, PAHs and EPFRs) all showed the lowest concentrations in summer and

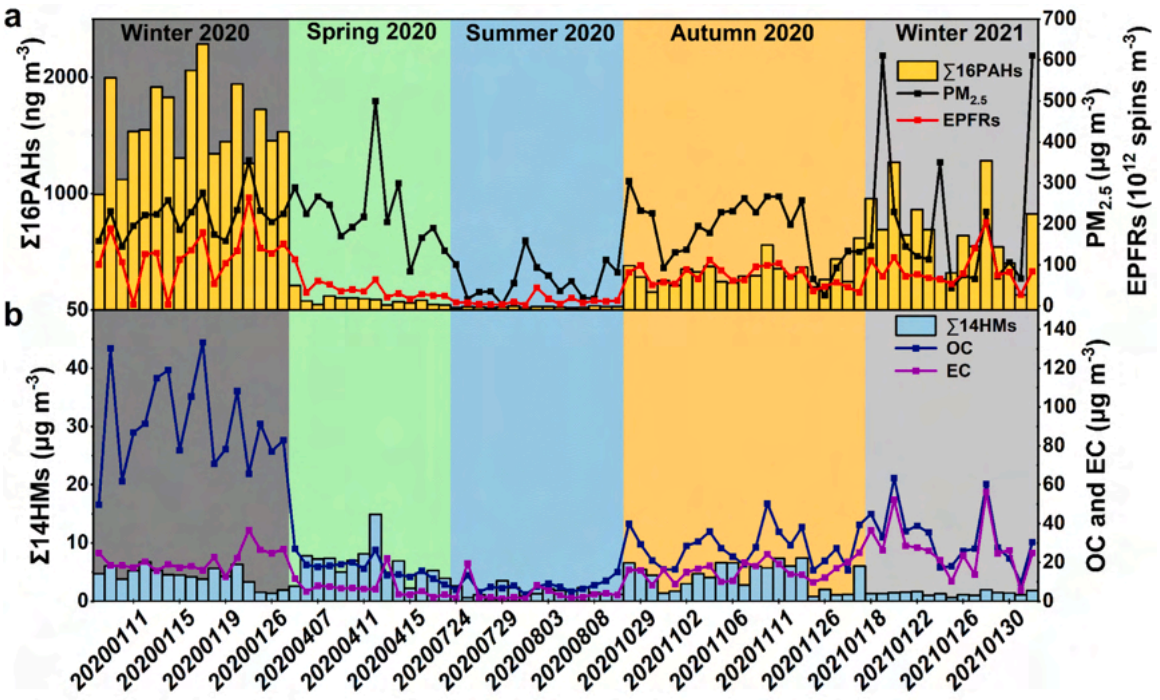


**Fig. 1.** Temporal variations of the concentrations of total PAHs (∑16 PAHs), $PM_{2.5}$ and EPFRs (a), and total heavy metals (∑14 HMs), OC and EC (b) in the sampling periods in 2020–2021.

**Table 1**
Concentrations (mean±standard deviation) of $PM_{2.5}$, total PAHs (∑16 PAHs), total heavy metals (∑14 HMs), EPFRs, OC and EC as well as indicators of health risks in the sampling periods in 2020–2021.

| Pollutants[a] | Winter 2020 | Spring 2020 | Summer 2020 | Autumn 2020 | Winter 2021 | Overall |
|---|---|---|---|---|---|---|
| $PM_{2.5}$ | 217.9 ± 48.7 | 227.5 ± 94.2 | 60.2 ± 41.9 | 185.1 ± 74.4 | 199.1 ± 181.6 | 178.9 ± 114.5 |
| ∑16 PAHs | 1605.1 ± 346.4 | 86.0 ± 42.5 | 25.6 ± 5.0 | 320.2 ± 110.4 | 671.4 ± 323.2 | 557.0 ± 617.6 |
| ∑14 HMs | 12.9 ± 4.6 | 18.9 ± 9.0 | 5.0 ± 2.4 | 13.0 ± 6.7 | 4.1 ± 1.0 | 10.9 ± 7.7 |
| EPFRs | 121.5 ± 60.9 | 41.6 ± 24.2 | 11.4 ± 10.3 | 71.6 ± 22.8 | 88.7 ± 40.3 | 68.9 ± 51.9 |
| EPFR g-factor | 2.00290 | 2.00287 | 2.00298 | 2.00287 | 2.00281 | 2.00288 |
| EPFR $\Delta H_{p\text{-}p}$ | 4.3 ± 0.4 | 4.5 ± 0.3 | 5.2 ± 1.5 | 4.5 ± 0.2 | 4.3 ± 0.3 | 4.5 ± 0.8 |
| OC | 90.9 ± 23.5 | 17.1 ± 5.0 | 7.9 ± 3.0 | 28.0 ± 9.2 | 32.7 ± 14.4 | 36.4 ± 32.1 |
| EC | 21.1 ± 5.5 | 7.0 ± 4.8 | 4.1 ± 4.5 | 15.6 ± 4.6 | 26.9 ± 13.1 | 15.2 ± 10.8 |
| $BaP_{teq}$ | 108.0 ± 22.1 | 10.0 ± 4.7 | 2.9 ± 0.9 | 33.0 ± 12.0 | 50.0 ± 24.3 | 42.2 ± 40.7 |
| $BaP_{meq}$ | 119.1 ± 25.0 | 11.5 ± 5.3 | 3.8 ± 1.3 | 36.7 ± 13.3 | 54.2 ± 26.2 | 46.7 ± 44.4 |
| $EQ_{cig}$ | 3.9 ± 2.0 | 1.3 ± 0.8 | 0.4 ± 0.3 | 2.3 ± 0.7 | 2.9 ± 1.3 | 2.2 ± 1.7 |

[a] $PM_{2.5}$, OC, EC and ∑14 HMs concentrations in μg $m^{-3}$, ∑16 PAHs, $BaP_{teq}$, and $BaP_{meq}$ in ng $m^{-3}$, EPFRs in $10^{12}$ spins $m^{-3}$, and $EQ_{cig}$ in person$^{-1}$ day$^{-1}$.

elevated concentrations in the cold seasons, particularly in winter due to the intensified domestic heating activities. It is interesting to note that the OC as well as PAH and EPFR concentrations in winter, 2020 were much higher than those in winter, 2021, while the EC concentrations in the two sampling periods in winter were similar. The average OC/EC ratio in the winters of 2020 and 2021 was 4.3 and 1.2, respectively, showing significantly higher OC/EC values in winter, 2020 than those in winter, 2021. The OC/EC ratio of particles originated from coal combustion is typically lower than that of particles from biomass burning. Besides, previous studies have shown that the OC/EC ratio could be smaller than 2 for carbonaceous aerosols dominated by the high temperature coal-fired sources [2] and greater than 4 for those from household coal or biomass burning [22]. With the outbreak of COVID-19 pandemic in January, 2020, people stayed at home all day without outside activities or work due to quarantine. Therefore, the need for household coal or biomass burning for heating was greatly increased in Ger area in particular, which consequently led to the significantly elevated OC emissions in January, 2020.

Fig. 2 shows the Spearman correlation coefficients among different species in $PM_{2.5}$, gaseous pollutants and meteorological parameters. While the carbonaceous species of $PM_{2.5}$ (OC, EC, PAHs and EPFRs) were generally highly intercorrelated, both PAHs and EPFRs showed stronger positive correlations with OC (r: 0.96 for ∑16 PAHs and r: 0.79 for EPFRs) than those with EC (r: 0.80 for ∑16 PAHs and r: 0.68 for EPFRs). Heavy metals were weakly correlated with the carbonaceous species of $PM_{2.5}$, however, the correlation of ∑14 HMs with $PM_{2.5}$ were comparable to those of the carbonaceous species with $PM_{2.5}$, indicating the diverse sources of $PM_{2.5}$ and the significant roles of both heavy metals and carbonaceous species in $PM_{2.5}$ pollution in Ulaanbaatar. The emissions of the carbonaceous species would be greatly increased in the cold seasons due to the excessive burning of solid fuels, therefore, the carbonaceous species showed significant negative correlations with temperature. In comparison, heavy metals were not correlated with temperature, but were negatively correlated with relative humidity (r: −0.38), which was partly attributable to the fact that dust events usually occur in dry weather. The intercorrelations of EPFRs with PAHs and heavy metals are further discussed in Section 3.3.

### 3.1.2. *Seasonal variations of PAHs*

Similar to OC, the PAHs concentration was the lowest in summer and

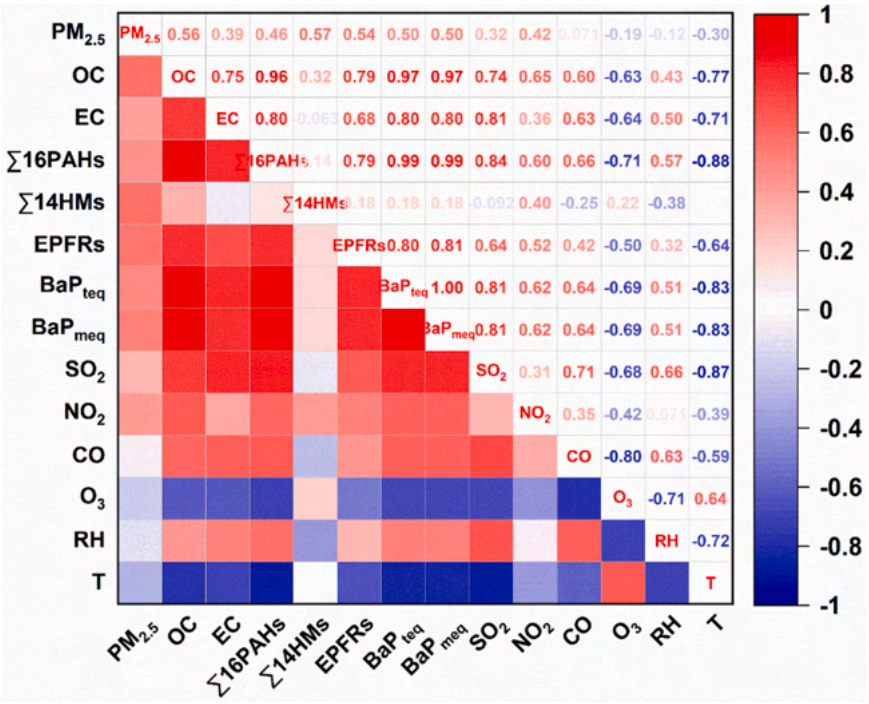


**Fig. 2.** Spearman correlation coefficients among different species in $PM_{2.5}$, gaseous pollutants and meteorological parameters.

became much higher in the cold seasons, especially in winter, 2020. Compared to the literature values, the concentration of $PM_{2.5}$-bound PAHs in Ulaanbaatar in the study period was at a high level compared to most other areas worldwide such as Beijing, China (305.91 ng $m^{-3}$) [23], Ceske Budejovice city, the Czech Republic (2.22 ng $m^{-3}$) [24] and Kanazawa, Japan (6.07 ng $m^{-3}$) [25], but lower than some other severely polluted areas such as Agra, India (2658 ng $m^{-3}$) [26] and Giza, Arabia (4342.30 ng $m^{-3}$) [27]. Fig. 3 shows the mean concentrations as well as molecular weight distributions of the 16 PAH monomers in the five sampling periods. Phe, Pyr, and Flt were the three most abundant PAHs in both winters (Fig. 3 and Table S1), which are typically emitted from coal combustion and biomass burning [2]. The medium molecular weight (MMW, 4 rings) PAHs therefore showed the highest percentage in the two winters, followed by the low molecular weight (LMW, 2–3 rings) PAHs. Compared to the LMW and MMW PAHs, the high molecular weight (HMW, 5–6 rings) PAHs are more closely related to vehicular emission [2]. The HMW PAHs showed the highest percentage in summer when the total PAH concentration was the lowest, which could be attributable to the reduced PAH emissions from the heating activities and the higher tendency of the LMW and MMW PAHs to partition into the gas phase [2,21].

### 3.1.3. *Seasonal variations of heavy metals*

Different from the carbonaceous species, the total heavy metal concentration in $PM_{2.5}$ in Ulaanbaatar was higher in spring and autumn rather than winter, probably due to the more frequent occurrence of dust events in spring and autumn [28]. However, the seasonal variation of total heavy metal concentration was less significant as compared to that of organic species such as PAHs and EPFRs, as shown in Fig. 1 and Table 1. The concentrations of toxic heavy metals such as As, Cd, Cr, Mn,

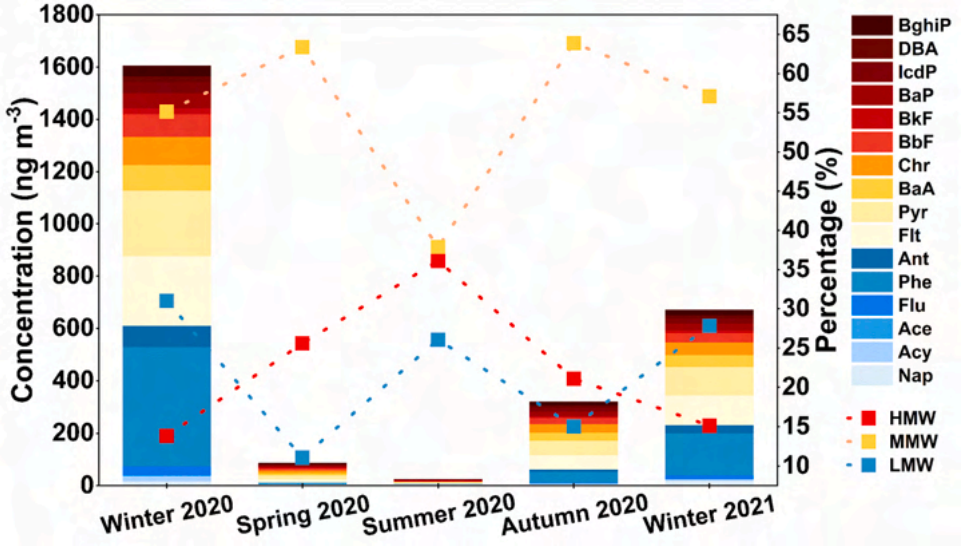


**Fig. 3.** PAH profiles and molecular weight distributions in the five sampling periods (HMW: 5–6 rings, MMW:4 rings, LMW: 2–3 rings).

Ni, and Pb often exceeded the limits set by the World Health Organization (WHO) and the European Commission (EC) during the five sampling periods (Table S2), indicating a severe heavy metal pollution in $PM_{2.5}$ in Ulaanbaatar all year round [36]. Fig. 4 shows the mean concentrations of the 14 heavy metals in each and the whole sampling periods. Fe was the most abundant metal (annual mean: 8796.4 ng $m^{-3}$) in $PM_{2.5}$, followed by Ba (annual mean: 595.6 ng $m^{-3}$), Zn (annual mean: 565.7 ng $m^{-3}$) and Mn (annual mean: 281.8 ng $m^{-3}$). As shown in Fig. 4, the concentrations of Fe and Mn were the highest in spring, which largely contributed to the elevated total concentration of ∑14 HMs in spring. Fe and Mn are typically abundant in soil dust [29], therefore, their high concentrations in $PM_{2.5}$ can be used to indicate the high contribution of soil dust to $PM_{2.5}$.

### 3.1.4. Seasonal variations of EPFRs

The EPFR concentration in $PM_{2.5}$ in Ulaanbaatar ranged from $2.2 \times 10^{12}$ to $264.0 \times 10^{12}$ spins $m^{-3}$ on a yearly basis, and the seasonal variation trend was similar to that of OC and PAHs with winter > autumn > spring > summer (Fig. 1 and Table 1). As shown in Fig. 5, the EPFR mean concentration was the highest in winter, 2020 ($121.5 \times 10^{12}$ spins $m^{-3}$), around an order of magnitude higher than that in summer ($11.4 \times 10^{12}$ spins $m^{-3}$), showing serious EPFR pollution in $PM_{2.5}$ in Ulaanbaatar due to the burning of solid fuels for heating. Similarly, Ahmad et al. reported noticeably higher concentrations of EPFRs in winter ($1.2 \times 10^{14}$ spin $m^{-3}$) than in summer ($1.7 \times 10^{13}$ spin $m^{-3}$) in Lahore, Pakistan, attributing the concentration fluctuations to changing weather conditions, industrial operations, and vehicular emissions [43]. Although the formation of EPFRs under ambient conditions could be facilitated with elevated temperature and solar radiation in summer [7], the potential increase of secondary EPFRs in summer was apparently overwhelmed by the significant increase of EPFRs directly released from the enhanced emission sources in winter.

Fig. 5 also shows the seasonal variation of EPFR g-factor (Fig. 5c) and line width (Fig. 5d) during the sampling period. Previous studies have reported that the g-factors of carbon-centered radicals (e.g., aromatic hydrocarbon radicals) are less than 2.0030, while those of oxygen-centered radicals (e.g., phenoxyl radicals) are larger than 2.0040 [30]. Generally, higher g-factors indicate the presence of more oxygen-centered radicals [7]. As shown in Table 1, the mean values of EPFR g-factors were all smaller than 2.0030 in each sampling period, indicating the majority of carbon-centered free radicals in $PM_{2.5}$ in Ulaanbaatar. However, the g-factor was apparently higher in summer (2.00298) than in other seasons, which could be attributed to the more diverse sources of EPFRs in summer and particularly the enhanced secondary formation of more oxygen-centered EPFRs [7,11]. It is interesting to note that the EPFR g-factor in winter, 2020 (2.00290) was also higher than that in winter, 2021 (2.00281), which was probably due to the intensified household coal or biomass burning in winter, 2020. $\Delta H_{p\text{-}p}$ can be used to indicate the species richness of EPFRs. The $\Delta H_{p\text{-}p}$ of EPFRs in $PM_{2.5}$ in Ulaanbaatar was the smallest in winter (4.3 G in both winters) and the largest in summer (5.2 G), suggesting a narrow range of sources in winter and a greater variety of sources in summer [7]. Sun et al. investigated the impact of domestic heating on EPFR pollution in a northern Chinese city (Yuncheng), and reported similar temporal variations of $\Delta H_{p\text{-}p}$ with a smaller $\Delta H_{p\text{-}p}$ (5.5 G) in the heating period than the non-heating period (5.7 G) [2].

### 3.1.5. Health risk assessment

The equivalent number of cigarettes ($EQ_{cig}$) based on EPFR concentrations and the total carcinogenic ($BaP_{teq}$) and mutagenic ($BaP_{meq}$) equivalent concentrations of PAHs are used to evaluate the health risks of $PM_{2.5}$ in Ulaanbaatar. As shown in Table 1, the average EQcig during the whole sampling period (2.2 $person^{-1}$ $day^{-1}$) was significantly higher than the EPA standard (0.4 $person^{-1}$ $day^{-1}$), with the highest in winter, 2020 (3.9 $person^{-1}$ $day^{-1}$) and the lowest in summer (0.4 $person^{-1}$ $day^{-1}$). $BaP_{teq}$ and $BaP_{meq}$ showed similar seasonal variations to $EQ_{cig}$, with an average of 42.2 ng $m^{-3}$ and 46.7 ng $m^{-3}$ in the whole sampling period, respectively. The significantly elevated $EQ_{cig}$, $BaP_{teq}$, and $BaP_{meq}$ in the cold seasons again highlighted the serious $PM_{2.5}$ pollution and the associated high health risks in Ulaanbaatar due to the burning of solid fuels for domestic heating.

The incremental lifetime cancer risks (ILCR) of PAHs and heavy metals were also calculated to show the long-term health risks of $PM_{2.5}$ in Ulaanbaatar (Table S3). According to the US EPA, an ILCR smaller than $10^{-6}$ suggests an acceptable cancer risk and no further action is required, an ILCR greater than $10^{-4}$ suggests an unacceptably high cancer risk, and an ILCR between $10^{-6}$ and $10^{-4}$ indicates a potential cancer risk [2,42]. The ILCR of all the carcinogenic pollutants investigated in this study exceeded the threshold of $10^{-6}$, and the order of carcinogenic risks was As > Cr(VI) > ∑16 PAHs > Cd > Co > Pb > Ni. In particular, the ILCR of As for adult male, adult female and children were $149.7 \times 10^{-6}$, $141.9 \times 10^{-6}$, and $114.8 \times 10^{-6}$, respectively, which were all above $10^{-4}$ and indicated an unacceptably high carcinogenic risk of As in $PM_{2.5}$ in Ulaanbaatar. Therefore, special attention should be paid to the effective control of heavy metals in $PM_{2.5}$ in this region, particularly those with high carcinogenic risks such as As and Cr (VI).

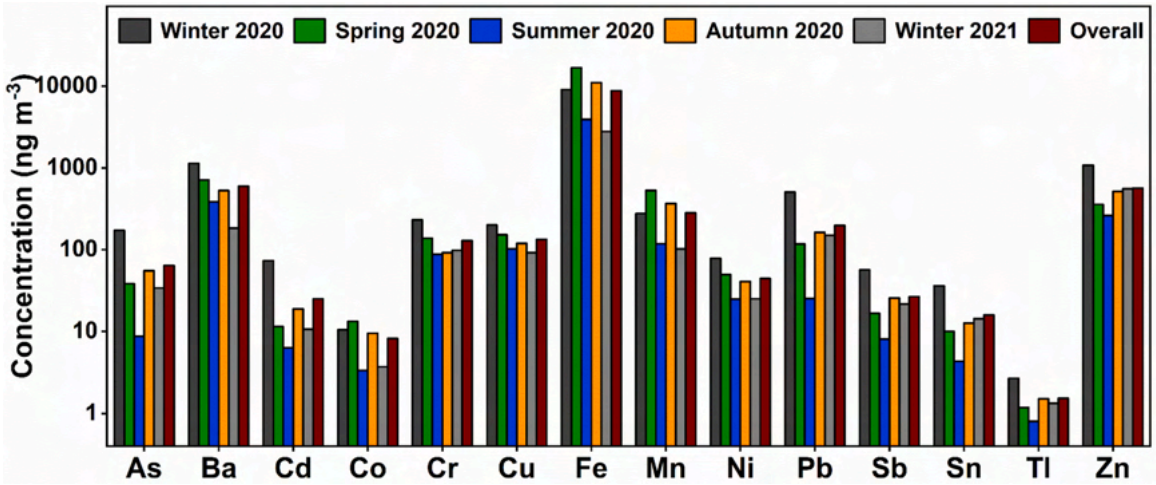


**Fig. 4.** Heavy metal profiles in $PM_{2.5}$ in each and the whole sampling periods.

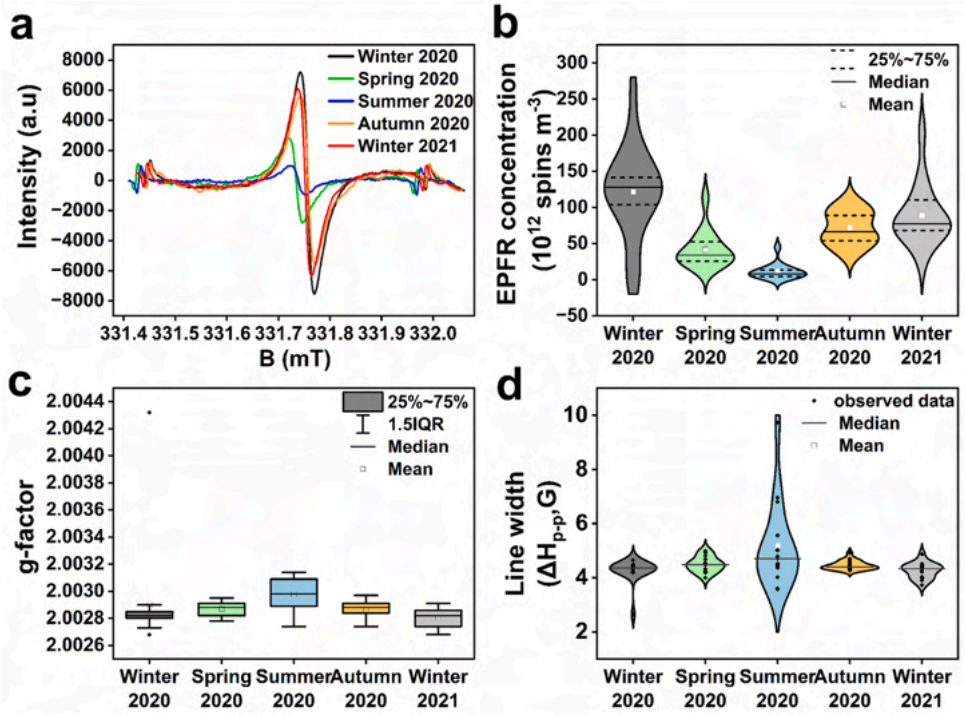


**Fig. 5.** The spectra (a), concentration (b), g-factor (c), and line width (d) of EPFRs measured by EPR during the sampling periods in four seasons.

### 3.2. Source apportionment of PAHs, heavy metals and EPFRs

#### 3.2.1. Diagnostic ratios of PAHs

Multiple diagnostic ratios of PAHs were readily calculated to qualitatively analyze the sources of PAHs in the five sampling periods [2]. As shown in Fig. 6, the diagnostic ratios of PAHs in autumn and winter overlap greatly, showing dominant contributions from the petroleum or coal/biomass combustion processes. The diagnostic ratios of PAHs in summer were uniquely different from those of PAHs in other seasons. The Ant/(Ant+Phe) and Flt/(Flt+Pyr) ratios in summer were less than

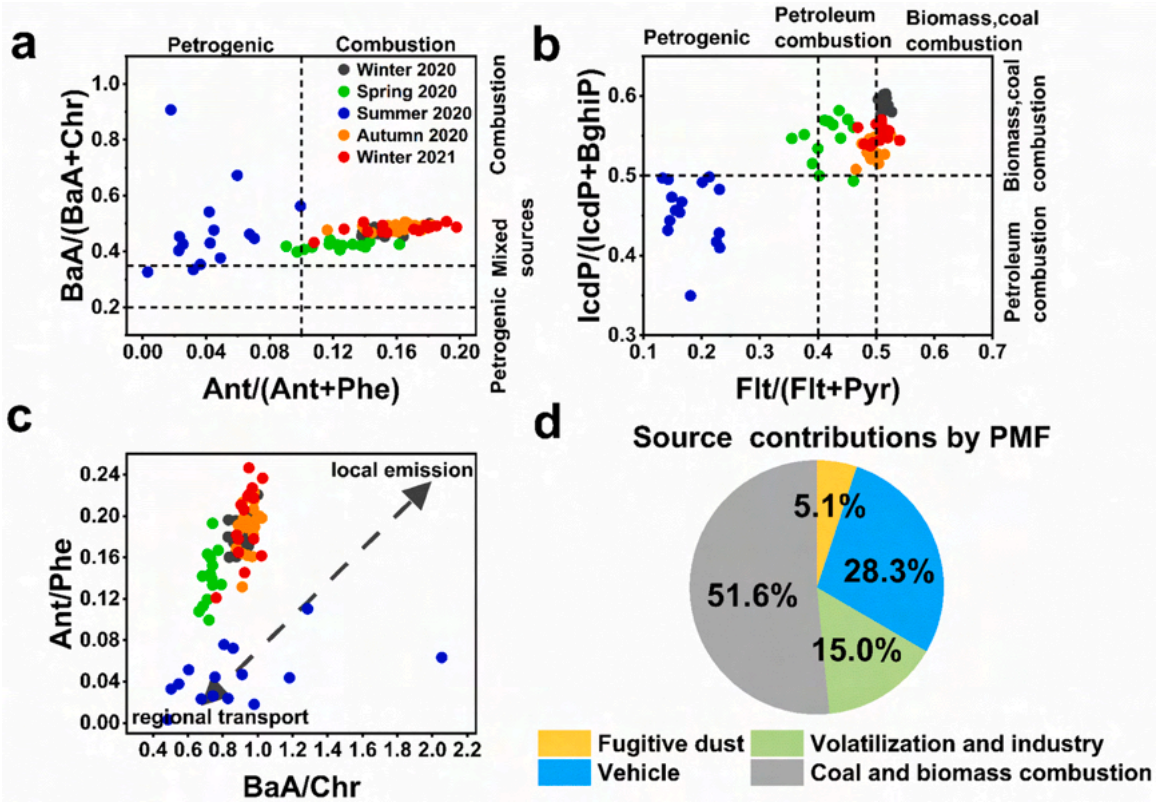


**Fig. 6.** Multiple diagnostic ratios of PAHs in the five sampling periods (a, b, and c) and source contributions of PAHs in the whole study period resolved by PMF (d).

0.1 and 0.4, respectively, indicating significant contributions of volatile petrogenic sources [37,38]. In addition, the BaA/(BaA+Chr) ratio was generally greater than 0.35 and the IcdP/(IcdP+BghiP) ratio was less than 0.5 in summer, designating petroleum combustion as another important source of PAHs in summer [39]. Fig. 6d also shows the source contributions of PAHs resolved by PMF on a yearly basis. Overall, the qualitative source analysis results based on the diagnostic ratios of PAHs were consistent with the source apportionment results by PMF, showing coal and biomass combustion as well as vehicular emission as the major sources of PAHs in $PM_{2.5}$ in Ulaanbaatar. Details of the PMF results are provided in Section 3.2.2.

The ratios of highly reactive PAHs to less reactive PAHs (such as Ant/Phe, BaA/Chr and BaP/BeP) can be used to determine whether the collected aerosols are fresh or aged, thus indicating the relative importance of local emissions versus regional transport [31,40]. Fig. 6c presents the variations of Ant/Phe and BaA/Chr in four seasons. The ratios of Ant/Phe and BaA/Chr were relatively low in summer and increased in the order of summer, spring, autumn and winter, indicating increased contributions from local emission as the weather became colder. The potential source regions of $PM_{2.5}$ in Ulaanbaatar in four seasons were also analyzed by PSCF and shown in Fig. S1. Overall, the major source areas that showed high WPSCF values were more distributed in the surrounding areas in winter than in summer, which is consistent with the diagnostic ratio results of PAHs shown in Fig. 6c. While the adjacent areas to the west of Ulaanbaatar were the major source regions of PAHs in winter, the summertime PAHs can originate from the directions of west, north or southeast. In addition to local emissions, long-distance transport of $PM_{2.5}$ also exerted a certain impact on $PM_{2.5}$ pollution in Ulaanbaatar, in which southern Russia and western Mongolia were important source regions of significant impact.

### 3.2.2. *Source apportionment by PMF*

PAH monomers and metal elements could serve as effective source tracers of $PM_{2.5}$ and its components duo to their unique emission characteristics from different sources and their stability in $PM_{2.5}$ [1,2]. In this study, the 16 PAH monomers and 14 heavy metals were employed as source tracers to apportion the sources of PAHs, heavy metals and EPFRs respectively by PMF. The respective source profiles for PAHs, heavy metals and EPFRs are presented in Figs. S2-S4. Four sources in total were resolved by PMF, including fugitive dust, vehicular emission, volatilization and industry, and coal and biomass combustion. The rationale for source identification is provided in the supporting file (Text S2).

Fig. 7 shows the annual and seasonal source contributions of PAHs, heavy metals and EPFRs in $PM_{2.5}$ in Ulaanbaatar in the sampling period of 2020–2021. According to the PMF calculation, the major sources of PAHs, EPFRs, and heavy metals varied greatly in Ulaanbaatar. On a yearly basis, coal and biomass combustion, vehicular emission, and fugitive dust were the dominant sources of PAHs, EPFRs, and heavy metals, respectively, accounting for 51.6 %, 56.4 %, and 58.0 % of the total source contributions for each species, respectively. The contribution of coal and biomass combustion to PAHs in winter was significantly higher than that in other seasons, particularly in the winter of 2020 (60.4 %), because coal as well as biomass was the main energy source for heating in the cold seasons of Ulaanbaatar. Vehicular emission was the second largest source to PAHs during the whole sampling period (28.3 %), and its contribution was amplified and stood out in autumn (46.2 %). Volatilization and industry became the dominant source of PAHs in the warmer seasons of summer (51.5 %) and spring (39.8 %), when the total PAH concentration was relatively low (Table 1). In comparison, Sun et al. reported volatilization (32.5 %) and coal combustion (47.5 %) as the dominant sources of $PM_{2.5}$-bound PAHs in a northern city (Yuncheng) of China during the non-heating and heating periods in winter, respectively [2].

Compared to PAHs that were largely derived from coal and biomass combustion in Ulaanbaatar, the major source of EPFRs was vehicular emission (56.4 %), followed by coal and biomass combustion (16.5 %), fugitive dust (15.5 %), and volatilization and industry (11.6 %). It is interesting to note that fugitive dust was the dominant source of EPFRs in spring (52.3 %), indicating a potentially high health risk of dust

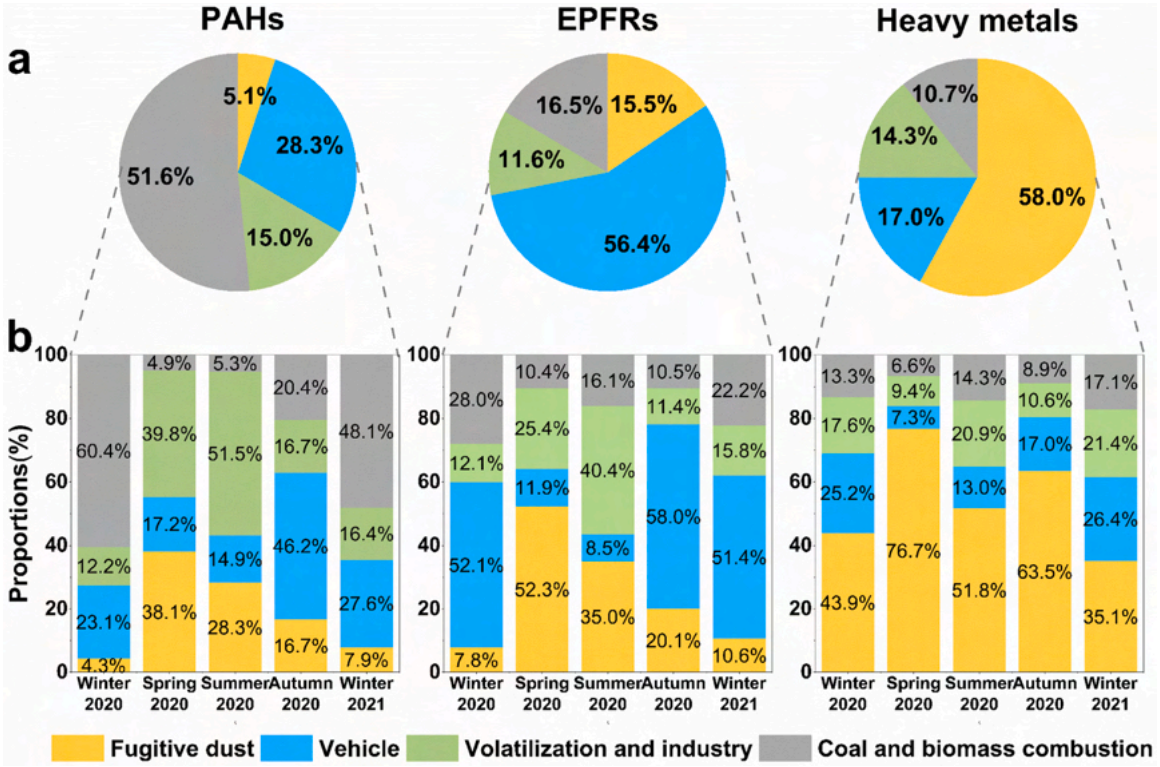


**Fig. 7.** Source contributions of PAHs, heavy metals and EPFRs in $PM_{2.5}$ in Ulaanbaatar in the whole (a) and each (b) sampling periods.

events. A previous study also reported elevated EPFR concentrations in $PM_{2.5}$ in Asian dust storms in spring, which contributed to the enhanced oxidative stress of $PM_{2.5}$ [12]. Although lower than in other seasons, the EPFR concentration was still substantially high in summer ($11.4 \times 10^{12}$ spins $m^{-3}$, Table 1), with major contributions from volatilization and industry (40.4 %) and fugitive dust (35.0 %). Employing PAHs and heavy metals as the source tracers of EPFRs, the calculated source contributions by PMF virtually comprised both the contributions from direct emissions and those of the subsequent secondary formation [2]. While the secondary formation of EPFRs could be diminished in the cold seasons [32], secondary formation may pose significant impact on EPFR pollution in summer.

Fugitive dust was straightly the dominant source of heavy metals in $PM_{2.5}$ in Ulaanbaatar all the year round, showing an overwhelming contribution in spring (76.7 %) due to frequent dust events. Given the high concentrations and significant health risks of heavy metals in Ulaanbaatar as shown in Table 1 and Table S3, the effective control of fugitive dust would be a promisingly efficient method in reducing $PM_{2.5}$ as well as its health risks in Ulaanbaatar. In addition to dust, vehicular emission was another important source of heavy metals in Ulaanbaatar, highly contributing to the toxic and carcinogenic species including As, Cd, and Pb (Fig. S3 and Fig. 7).

### 3.3. Intercorrelations of EPFRs with PAHs and heavy metals

PAHs and several metal oxides such as CuO, ZnO, and $Fe_2O_3$ have been identified as important organic precursors and surface catalysts, respectively, for EPFR formation through simulated combustion experiments [9,14]. However, the interactions among PAHs, metals, and EPFRs in the real atmosphere have been rarely proved in previous field studies. Overall, EPFRs showed the highest correlation with OC (r: 0.79) and ∑16 PAHs (r: 0.79), followed by that with EC (r: 0.68) and $PM_{2.5}$ (r: 0.54), as shown in Fig. 2. Besides, the correlations between EPFRs and the gaseous pollutants followed the order of $SO_2$ (r: 0.64) > $NO_2$ (r: 0.52) > CO (r: 0.42). In a recent study in Fairbanks, Alaska, a different correlation pattern was observed between EPFRs and the related pollutants, with a stronger correlation of EPFRs with EC ($R^2$: 0.79) than OC ($R^2$: 0.64) and a stronger correlation of EPFRs with CO ($R^2$: 0.75) than $NO_2$ ($R^2$: 0.63) or $SO_2$ ($R^2$: 0.43) [32]. Such difference could be explained by the different source contributions of EPFRs in the two study aeras: in addition to the common source of vehicular emission, coal and biomass combustion contributed significantly to EPFRs in Ulaanbaatar while the major source of EPFRs in Fairbanks, Alaska was the incomplete combustion of residential wood burning [32].

While strong correlations between EPFRs and PAHs have been observed in the current as well as previous field studies [2,32], EPFRs were found to be weakly linked to ∑14 HMs (r: 0.18), as shown in Fig. 2. Since ∑14 HMs was a composite of 14 heavy metals of distinctly different natures and sources, the relationship of EPFRs and each heavy metal was further investigated. Fig. 8 shows the Spearman correlation coefficients of EPFRs with each heavy metal as well as PAH monomer in $PM_{2.5}$. Overall, EPFRs were significantly correlated with most PAHs, with slightly stronger correlations with PAHs originating from vehicular emission than with those from coal and biomass combustion. However, the correlations of EPFRs with different heavy metals varied greatly. As shown in Fig. 8, EPFRs were significantly correlated with Zn, Pb, Sb, Sn, Tl as well as As and Cd, but weakly correlated with Fe, Mn, Ba, Co, Cr, Cu, and Ni. It appears that heavy metals contained in soil dust, such as Fe, Mn, Co and Ba, showed the least association with EPFRs. However, EPFRs showed no preference with heavy metals originating from the other three sources. Instead, the order of correlation strength between EPFRs and the rest heavy metals seems to follow the order of oxidizing strength of the corresponding metal cations, as indicated by their order in the periodic table [14]. Based on a series of thermochemical reactions of PAH derivatives catalyzed by various metal oxides, Yang et al. reported that the catalyzing abilities of metal oxides for EPFR formation

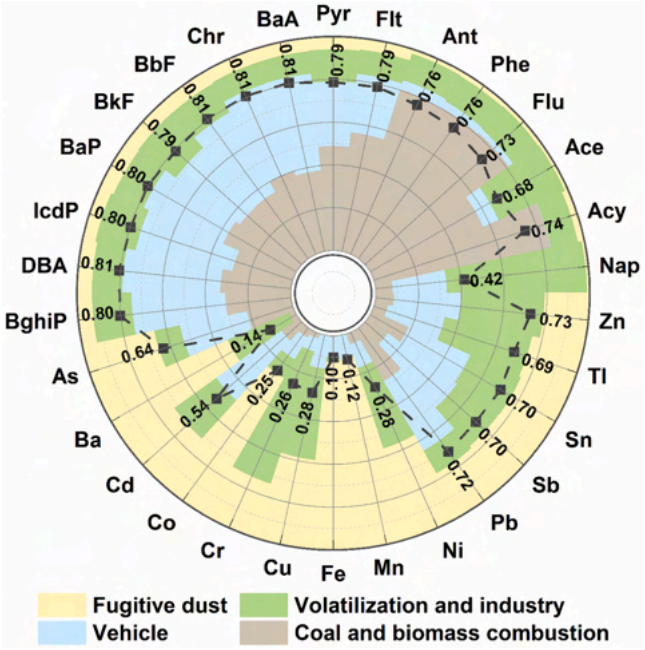


**Fig. 8.** Spearman correlation coefficients of EPFRs with PAHs and heavy metals in $PM_{2.5}$ in Ulaanbaatar. Contributions of different sources to each species are marked in colors.

were in the order of ZnO > CuO > NiO, which was in accordance with the order of correlation strength between EPFRs and the related heavy metals in this field observation [14].

Previous laboratory simulation or field studies have shown that EPFRs could be formed via either electron migration between PAHs and transition metal oxides on particles formed during heating or combustion [14,33], or through photochemical reactions of PAHs themselves that may not be mediated by transition metals [34,35]. The strong correlations of EPFRs with PAHs in this study also suggest that PAHs may act as an important group of organic precursors for EPFR formation. On the other hand, the significant correlations between EPFRs and several heavy metals indicate that transition metals such as Zn, Pb, Sb, Sn, Tl may also play an important role in the formation of EPFRs. The dominant contribution of vehicles to EPFR pollution in $PM_{2.5}$ in Ulaanbaatar could be due to the co-emissions of PAHs and specific heavy metals in vehicular emission. Besides, those heavy metals that show significant correlations with EPFRs may also catalyze the photochemical formation of EPFRs under ambient conditions, as indicated by their various sources that differ greatly from the sources of organic precursors such as PAHs. Such hypothesis needs to be further confirmed by photochemical simulation experiments that employ proper organic precursors and transition metal oxides such as those suggested in this study.

## 4. Conclusions and environmental implications

The use of coal for household heating in Ulaanbaatar particularly in the Ger area has led to extreme air pollution problems. In the study period in 2020–2021, Ulaanbaatar was severely polluted with $PM_{2.5}$ in most seasons except for summer, with the mean $PM_{2.5}$ concentration over 150 μg $m^{-3}$. The toxic organic pollutants such as PAHs showed elevated concentrations in the cold seasons as a result of the domestic heating activities, highlighting the urgent demand of clean energy for heating. Moreover, in the context of climate change and the more frequent occurrence of dust events, metal elements that are highly associated with dusts would exert significant health effects on local residents. Therefore, special attention should also be paid to the effective control of heavy metals in $PM_{2.5}$, such as As and Cr(VI) that

exhibited high carcinogenic risks. Similar to the case in Ulaanbaatar, many areas worldwide are suffering from severe air pollution resulted from solid fuel burning as well as dust events, and the results of this study would be of direction implications for local actions regarding air quality improvement and health risk reduction.

Different from PAHs and heavy metals, vehicular emission was the major source of EPFRs in Ulaanbaatar (56.4 %), followed by coal and biomass combustion (16.5 %), fugitive dust (15.5 %), and volatilization and industry (11.6 %). EPFRs were highly correlated with most PAHs, particularly those from vehicular emission. Besides, EPFRs were significantly correlated with Zn, Pb, Sb, Sn, Tl as well as As and Cd, but weakly correlated with metal elements that were dominantly contained in soil dust. According to the intercorrelations of EPFRs with PAHs and heavy metals from different sources, the dominant contribution of vehicular emission to EPFR pollution in $PM_{2.5}$ in Ulaanbaatar could be largely attributed to the co-emissions of PAHs and specific heavy metals in vehicular emission. It should be noted that it is virtually difficult to explore the mechanistic details of the interactions between EPFRs and other pollutants merely through field observation and correlation analysis. Well designed orthogonal experiments employing proper organic precursors and transition metal oxides are needed to mechanistically explore the interactions among PAHs, metals, and EPFRs in the atmosphere and the resulting health impact. Interdisciplinary approaches that could incorporate atmospheric chemistry, toxicology, and public health studies are encouraged to broaden the understanding of EPFR dynamics.

## Environmental Implication

Many areas worldwide are still heavily dependent on solid fuels for domestic heating, releasing large amounts of $PM_{2.5}$ and the associated toxic pollutants. This study simultaneously investigated the characteristics, health risks and sources of PAHs, heavy metals and EPFRs in Ulaanbaatar, Mongolia, which is one of the coldest and most polluted capital cities in the world. This comprehensive study of PAHs, heavy metals and EPFRs in $PM_{2.5}$ further provides direct evidence on the intercorrelations of the three toxic species and elucidates the effects of different PAHs and heavy metals on EPFR formation.

## CRediT authorship contribution statement

**Shihan Wu**: Methodology, Investigation, Validation, Formal analysis, Writing – original draft, Visualization. **Ke Xin**: Methodology, Investigation, Validation, Formal analysis. **Jing Chen**: Supervision, Conceptualization, Writing – review & editing, Visualization, Project administration, Funding acquisition. **Narmandakh Dambajamts**: Investigation. **Yuewei Sun**: Investigation. **Jing Ai**: Investigation. **Wei Ouyang**: Conceptualization, Investigation. **Bilguun Ulziibat**: Investigation. **Enkh-Uchral Batkhuyag**: Investigation. **Soyol-Erdene Tseren-Ochir**: Conceptualization, Methodology, Investigation.

## Declaration of Competing Interest

The authors declare that they have no known competing financial interests or personal relationships that could have appeared to influence the work reported in this paper.

## Acknowledgments

The present work was financially supported by National Key R&D Program of Intergovernmental International Science and Technology Innovation Cooperation, China (2023YFE0100200), Asia Pacific Network grant (CRECS2020–01MY-Tseren-Ochir) and the research grant of the National University of Mongolia (P2023–4606). The graduate students' scholarship from Ministry of Environment and Tourism of Mongolia was supported for Bilguun Ulziibat (MNG-RS-004).

## Appendix A. Supporting information

Supplementary data associated with this article can be found in the online version at doi:10.1016/j.jhazmat.2025.137586.

## Data Availability

Data will be made available on request.

## References

[1] Ahmad, M., Yu, Q., Chen, J., Cheng, S., Qin, W., Zhang, Y., 2021. Chemical characteristics, oxidative potential, and sources of PM2.5 in wintertime in Lahore and Peshawar, Pakistan. J Environ Sci 102, 148–158.
[2] Sun, Y., Chen, J., Qin, W., Yu, Q., Xin, K., Ai, J., Huang, H., Liu, X., 2022. Gas-PM2.5 partitioning, health risks, and sources of atmospheric PAHs in a northern China city: Impact of domestic heating. Environ Pollut 313.
[3] Kim, K., Jahan, S.A., Kabir, E., Brown, R.J.C., 2013. A review of airborne polycyclic aromatic hydrocarbons ( PAHs) and their human health effects. Environ Int 60, 71–80.
[4] Pateraki, S., Asimakopoulos, D.N., Maggos, T., Assimakopoulos, V.D., Bougiatioti, A., Bairachtari, K., Vasilakos, C., Mihalopoulos, N., 2020. Chemical characterization, sources and potential health risk of PM2.5 and PM1 pollution across the Greater Athens Area. Chemosphere 241.
[5] Tian, Y., Jia, B., Zhao, P., Song, D., Huang, F., Feng, Y., 2022. Size distribution, meteorological influence and uncertainty for source-specific risks: PM2.5 and PM10 -bound PAHs and heavy metals in a Chinese megacity during 2011 - 2021. Environ Pollut 312.
[6] Gao, Y., Guo, X., Ji, H., Li, C., Ding, H., Briki, M., Tang, L., Zhang, Y., 2016. Potential threat of heavy metals and PAHs in PM2.5 in different urban functional areas of Beijing. Atmos Res 178, 6–16.
[7] Ai, J., Qin, W., Chen, J., Sun, Y., Yu, Q., Xin, K., Huang, H., Zhang, L., Ahmad, M., Liu, X., 2023. Pollution characteristics and light-driven evolution of environmentally persistent free radicals in PM2.5 in two typical northern cities of China. J Hazard Mater 454.
[8] Zhang, Y., Xu, M., Liu, X., Wang, M., Zhao, J., Li, S., Yin, M., 2021. Regulation of biochar mediated catalytic degradation of quinolone antibiotics: important role of environmentally persistent free radicals. Bioresour Technol 326.
[9] Kelley, M.A., Hebert, V.Y., Thibeaux, T.M., Orchard, M.A., Hasan, F., Cormier, S.A., Thevenot, P.T., Lomnicki, S.M., Varner, K.J., Dellinger, B., Latimer, B.M., Dugas, T. R., 2013. Model combustion-generated particulate matter containing persistent free radicals redox cycle to produce reactive oxygen species. Chem Res Toxicol 26 (12), 1862–1871.
[10] Jia, H., Zhao, S., Shi, Y., Zhu, L., Wang, C., Sharma, V.K., 2018. Transformation of polycyclic aromatic hydrocarbons and formation of environmentally persistent free radicals on modified montmorillonite: the role of surface metal ions and polycyclic aromatic hydrocarbon molecular properties. Environ Sci Technol 52 (10), 5725–5733.
[11] Borrowman, C.K., Zhou, S., Burrow, T.E., Abbatt, J.P.D., 2016. Formation of environmentally persistent free radicals from the heterogeneous reaction of ozone and polycyclic aromatic compounds. Phys Chem Chem Phys 18 (1), 205–212.
[12] Chen, Q., Wang, M., Sun, H., Wang, X., Wang, Y., Li, Y., Zhang, L., Mu, Z., 2018. Enhanced health risks from exposure to environmentally persistent free radicals and the oxidative stress of PM2.5 from Asian dust storms in Erenhot, Zhangbei and Jinan, China. Environ Int 121, 260–268.
[13] Liu, S., Huang, W., Yang, J., Xiong, Y., Huang, Z., Wang, J., Cai, T., Dang, Z., Yang, C., 2023. Formation of environmentally persistent free radicals on microplastics under UV irradiations. J Hazard Mater 453.
[14] Yang, L., Liu, G., Zheng, M., Jin, R., Zhao, Y., Wu, X., Xu, Y., 2017. Pivotal roles of metal oxides in the formation of environmentally persistent free radicals. Environ Sci Technol 51 (21), 12329–12336.
[15] Sarmiento, D.J., Majestic, B.J., 2023. Formation of environmentally persistent free radicals from the irradiation of polycyclic aromatic hydrocarbons. J Phys Chem A 127 (25), 5390–5401.
[16] Cavanaugh, R., 2017. Extreme air pollution in Mongolia's overflowing capital. Lancet Resp Med 5 (8), 614–615.
[17] Cousins, S., 2019. Air pollution in Mongolia. Bull World Health Organ 97 (2), 79–80.
[18] Ahmad, M., Cheng, S., Yu, Q., Qin, W., Zhang, Y., Chen, J., 2020. Chemical and source characterization of PM2.5 in summertime in severely polluted Lahore, Pakistan. Atmos Res 234.
[19] Gehling, W., Dellinger, B., 2013. Environmentally persistent free radicals and their lifetimes in PM2.5. Environ Sci Technol 47 (15), 8172–8178.
[20] Yu, Q., Chen, J., Qin, W., Cheng, S., Zhang, Y., Sun, Y., Xin, K., Ahmad, M., 2021. Characteristics, primary sources and secondary formation of water-soluble organic aerosols in downtown Beijing. Atmos Chem Phys 21 (3), 1775–1796.
[21] Zhang, Y., Chen, J., Yang, H., Li, R., Yu, Q., 2017. Seasonal variation and potential source regions of PM2.5 -bound PAHs in the megacity Beijing, China: impact of regional transport. Environ Pollut 231, 329–338.
[22] Vicente, E.D., Alves, C.A., 2018. An overview of particulate emissions from residential biomass combustion. Atmos Res 199, 159–185.
[23] Zhang, J., Yang, L., Mellouki, A., Chen, J., Chen, X., Gao, Y., Jiang, P., Li, Y., Yu, H., Wang, W., 2018. Atmospheric PAHs, NPAHs, and OPAHs at an urban,

mountainous, and marine sites in Northern China: molecular composition, sources, and ageing. Atmos Environ 173, 256–264.
[24] Polachova, A., Gramblicka, T., Parizek, O., Sram, R.J., Stupak, M., Hajslova, J., Pulkrabova, J., 2020. Estimation of human exposure to polycyclic aromatic hydrocarbons ( PAHs) based on the dietary and outdoor atmospheric monitoring in the Czech Republic. Environ Res 182.
[25] Zhang, X., Zhang, H., Wang, Y., Bai, P., Zhang, L., Toriba, A., Nagao, S., Suzuki, N., Honda, M., Wu, Z., Han, C., Hu, M., Tang, N., 2025. Estimation of gaseous polycyclic aromatic hydrocarbons ( PAHs) and characteristics of atmospheric PAHs at a traffic site in Kanazawa, Japan. J Environ Sci 149, 57–67.
[26] Verma, P.K., Sah, D., Satish, R., Rastogi, N., Kumari, K.M., Lakhani, A., 2022. Atmospheric chemistry and cancer risk assessment of Polycyclic Aromatic Hydrocarbons (PAHs) and Nitro-PAHs over a semi-arid site in the Indo-Gangetic plain. J Environ Manag 317.
[27] Hassan, S.K., Khoder, M.I., 2012. Gas-particle concentration, distribution, and health risk assessment of polycyclic aromatic hydrocarbons at a traffic area of Giza, Egypt. Environ Monit Assess 184 (6), 3593–3612.
[28] Zong, Q., Mao, R., Gong, D., Wu, C., Pu, B., Feng, X., Sun, Y., 2021. Changes in dust activity in spring over east asia under a global warming scenario. Asia-Pac J Atmos Sci 57 (4), 839–850.
[29] Dash, D., Mishra, H.K., 2023. Seasonal variation of water quality and heavy metal pollution index: a case study. Int J Ecol Dev 38 (2), 37–55.
[30] Dellinger, B., Loninicki, S., Khachatryan, L., Maskos, Z., Hall, R.W., Adounkpe, J., McFerrin, C., Truong, H., 2007. Formation and stabilization of persistent free radicals. Proc Combust Inst 31, 521–528.
[31] Ding, X., Wang, X., Xie, Z., Xiang, C., Mai, B., Sun, L., Zheng, M., Sheng, G., Fu, J., Poeschl, U., 2007. Atmospheric polycyclic aromatic hydrocarbons observed over the North Pacific Ocean and the Arctic area: spatial distribution and source identification. Atmos Environ 41 (10), 2061–2072.
[32] Edwards, K.C., Kapur, S., Fang, T., Cesler-Maloney, M., Yang, Y., Holen, A.L., Wu, J., Robinson, E.S., DeCarlo, P.F., Pratt, K.A., Weber, R.J., Simpson, W.R., Shiraiwa, M., 2024. Residential wood burning and vehicle emissions as major sources of environmentally persistent free radicals in fairbanks, Alaska. Environ Sci Technol 58 (32), 14293–14305.
[33] Xu, M., Wu, T., Tang, Y., Chen, T., Khachatryan, L., Iyer, P.R., Guo, D., Chen, A., Lyu, M., Li, J., Liu, J., Li, D., Zuo, Y., Zhang, S., Wang, Y., Meng, Y., Qi, F., 2019. Environmentally persistent free radicals in PM2.5: a review. Waste Dispos Sustain Energy 1 (3), 177–197.
[34] Chen, Q., Sun, H., Wang, M., Wang, Y., Zhang, L., Han, Y., 2019. Environmentally persistent free radical ( EPFR) formation by visible-light illumination of the organic matter in atmospheric particles. Environ Sci Technol 53 (17), 10053–10061.
[35] Zhu, K., Jia, H., Zhao, S., Xia, T., Guo, X., Wang, T., Zhu, L., 2019. Formation of environmentally persistent free radicals on microplastics under light irradiation. Environ Sci Technol 53 (14), 8177–8186.
[36] Khan, C., Malik, R.N., Chen, J., 2024. Human exposure to chromite mining pollution, the toxicity mechanism and health impact. Heliyon 10, e40083.
[37] Sankar, T.K., Kumar, A., Mahto, D.K., Das, K.C., Narayan, P., Fukate, M., Awachat, P., Padghan, D., Mohammad, F., Al-Lohedan, H.A.A., Soleiman, A.A.A., Ambade, B., 2023. The health risk and source assessment of polycyclic aromatic hydrocarbons (PAHs) in the soil of industrial cities in India. Toxics 11 (6).
[38] Ambade, B., Sethi, S.S., Chintalacheruvu, M.R., 2023. Distribution, risk assessment, and source apportionment of polycyclic aromatic hydrocarbons (PAHs) using positive matrix factorization (PMF) in urban soils of East India. Environ Geochem Health 45 (2), 491–505.
[39] Ambade, B., Sethi, S.S., Kurwadkar, S., Mishra, P., Tripathee, L., 2022. Accumulation of polycyclic aromatic hydrocarbons (PAHs) in surface sediment residues of Mahanadi River Estuary: Abundance, source, and risk assessment. Mar Pollut Bull 183.
[40] Ambade, B., Sethi, S.S., Giri, B., Biswas, J.K., Bauddh, K., 2022. Characterization, behavior, and risk assessment of polycyclic aromatic hydrocarbons (PAHs) in the estuary sediments. Bull Environ Contam Toxicol 108 (2), 243–252.
[41] Yu, Q., Chen, J., Cheng, S., Qin, W., Zhang, Y., Sun, Y., Ahmad, M., 2021. Seasonal variation of dicarboxylic acids in PM2.5 in Beijing: implications for the formation and aging processes of secondary organic aerosols. Sci Total Environ 763, 142964.
[42] Mehmood, T., Zhu, T., Ahmad, I., Li, X., 2020. Ambient PM2.5 and PM10 bound PAHs in Islamabad, Pakistan: concentration, source and health risk assessment. Chemosphere 257.
[43] Ahmad, M., Chen, J., Yu, Q., Khan, M.T., Ali, S.W., Nawab, A., Phairuang, W., Panyametheekul, S., 2023. Characteristics and risk assessment of environmentally persistent free radicals (EPFRs) of PM2.5 in Lahore, Pakistan. Int J Environ Res Public Health 20 (3), 2384.